Daniel E. Friedmann
MacDonald, Dettwiler & Associates Ltd.
Richmond, B.C. V6X 2Z9, Canada

Two-Dimensional Resampling of Line Scan Imagery by One-Dimensional Processing

One-dimensional processing makes digital image rotation possible by eliminating the large memory requirements and slow data access which accompany two-dimensional digital image rotation.

Abstract: *Geometric correction of remote sensing data, such as Landsat MSS data, requires two-dimensional resampling. The resampling operation is typically carried out in two one-dimensional operations: along and across scan lines. The usual reasons given for validating the procedure are lower cost and higher speed.*

The theoretical assumptions under which one-dimensional processing is valid are presented in the light of current and future remote sensing sensors. It is shown that the assumptions are violated when a substantial amount of image rotation is incorporated into the precision processing. A method to perform image rotation with an additional step using one-dimensional processing is presented. The method makes precision correction and alignment of remote sensing data, to a map projection, both possible and accurate with one-dimensional processing.

Introduction

The production of precision processed satellite imagery requires both precision rectification and photometric correction of pixel (picture element) intensities. Precision rectification involves two steps.

First, the internal error sources and external error sources are modeled by a two-dimensional transformation.

Second, the pixel intensities on a regular grid in the corrected projection are obtained. The required pixel coordinate in the corrected projection is mapped to the raw spacecraft projection (by means of the inverse transformation). The mapping usually yields non-integral positions in the raw projection; thus, the desired pixel intensity is obtained by interpolation on the known pixel intensities. This process is referred to as resampling. The geometric transformation[1-3] models internal errors such as scan nonlinearity and varying line length. It also models many external errors such as uncertainties in the spacecraft attitude, ephemeris, and terrain relief. The transformation also corrects for spacecraft heading and map projection. Heading correction refers to the rotation of the digital data by the spacecraft heading angle so that after precision rectification the data are aligned with the output map projection or geocoded. For example, if the image is corrected to the UTM map projection, the digital data lie along northings and eastings.

The increased number of satellites planned for the next decade,[4] and the increased amount of geocoded[5] digital data being made available, will make the production of geocoded images (heading correction) a necessity if data from different sources are to be compared and analyzed together as required for the successful application of remote sensing techniques.

The improved sensors to be carried by the new spacecraft[6-11] will demand accurate processing. Future scanners, such as the thematic mapper[6,11]

Photogrammetric Engineering and Remote Sensing,
Vol. 47, No. 10, October 1981, pp. 1459-1467.

0099-1112/81/4710-1459 $02.25/0

(Landsat) and multispectral linear[7-10,12] arrays (SPOT, Mapsat, LASS, COMSS, . . .), will make available to the user increased radiometric, spatial, and in some cases, spectral resolution. Processing must preserve the radiometric accuracy of the sensor.

The correct way to interpolate or resample two-dimensional digital data is with two-dimensional convolution (the application of a linear filter specified by its impulse response). In particular, if the data are band limited, the resampling kernel (or impulse response of the linear filter) is

$$g(x_1, x_2) = \frac{\sin \pi x_1}{\pi x_1} \cdot \frac{\sin \pi x_2}{\pi x_2} \qquad (1)$$

where x_1 and x_2 are the orthogonal axes along which the data are sampled.* In practice, application of two-dimensional convolution is slow and expensive, the tradeoff being between using large amounts of random access memory and suffering from slow access of data on disk.

The large volumes of remote sensing data (i.e., 40 MBytes per band for thematic mapper data) must be accessed from disk, line-by-line. This becomes even slower and more expensive[14] in image rotation which requires access to a large portion of the image for one output line (i.e., must traverse diagonally through the input data). When the data can be processed in a one-dimensional manner, the number of computations is reduced and the data access problem eased considerably.

One-dimensional processing for precision rectification of Landsat MSS data has been in use. It is the purpose of this paper to present the theoretical arguments for validating one-dimensional precision processing of imagery data from present and future sensors. Furthermore, it is shown how this processing must be modified from two one-dimensional operations (along and across scan lines) to *three* one-dimensional operations in order to incorporate image rotation by any angle. With the three-pass method it is possible to correct images to a geocoded format.

One-Dimensional Processing

The possibility of performing one-dimensional processing is strongly dependent on the nature of the satellite data, the nature of the inherent distortions, the final map projection, and the rotation process.

The following sections show why the data acquisition is inherently one-dimensional, how this leads to a separable resampling kernel†, and how a separable kernel can be used to perform two-dimensional resampling as a series of one-dimensional resamplings in the case of precision rectification with and without heading correction.

Satellite Sensors

Landsats 1, 2, and 3 have demonstrated the operational utility of remote sensing from space with the multispectral scanner (MSS). Future sensors appear to be scanners: initially, mechanical scanners, such as the Thematic Mapper (TM), and then electronic scanners, such as the multispectral linear arrays (MLA). Scanners have important processing implications. Before discussing these, it is instructive to examine a well-known scanner such as the MSS from the signal processing point of view (operational details, well covered in literature are omitted [15-19]).

Figure 1 shows a block diagram of the scanner system. The imagery data are imaged by the optical system (box 2, Figure 1) (a Ritchey Chretien telescope *f*/No. of 3.6) onto the focal plane. The imaging process low-pass filters (or smears) the data in both dimensions. The filtering action is best modeled by a Gaussian impulse response (blur circle 30 m[15]) which is separable. On the focal plane (box 3, Figure 1) the data are sampled vertically by the aperture stop (formed by square optical fibres in the case of MSS, except for the IR band) as the scanning mirror images a line of data. The aperture has the effect of averaging the intensity over the square which represents 76.2 m[15] on the ground. This low-pass filtering by a square aperture is separable. From now on the two-dimensional data are effectively a series of one-dimensional scan lines, and any further filtering affects only the along-scan spatial frequencies. After detection, accompanied by radiometric degradation of the data (box 4, Figure 1), the data are low-pass filtered (box 5, Figure 1) (three pole, Butterworth in the case of MSS) and sampled horizontally (box 6, Figure 1). The data, now digitized in the along- and across-scan direction, are quantized (64 levels for MSS) and transmitted (boxes 7, 8).

The scenario for TM is identical except for the increased resolution (spatial, radiometric, and spectral). For multispectral linear arrays the steps are similar except that the data are sampled horizontally by the thousands of detector apertures and vertically by electronic means (as the satellite progresses in its orbit).

The important points to realize from the above example for our purposes are

(1) Scanner data are inherently acquired by a one-dimensional process,
(2) The spatial filtering performed on the data is separable into two orthogonal directions,
(3) The data are rectangularly sampled in the same two directions, and
(4) The data are not band-limited in the Nyquist sense prior to sampling (i.e., the sampling rate is not high enough to avoid frequency ambiguity).

* See reference 13 for an extensive review of the two-dimensional sampling theorem.

† A function $g(x_1,x_2)$ is separable when $g(x_1,x_2) = g_1(x_1)\, g_2(x_2)$.

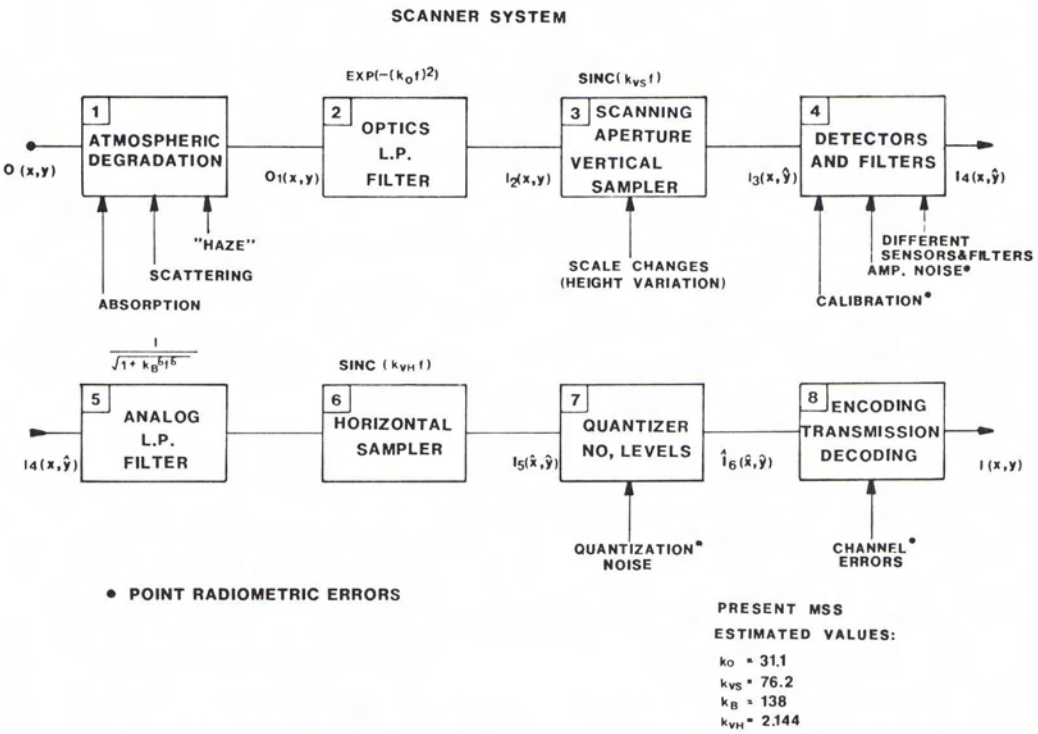

FIG. 1. Scanner imaging system. Functions and values are for the present MSS.

Since the filtering performed on the data is separable, the spatial frequencies of the data lie within a rectangle. However, a plot of the system modulation transfer function (MTF) prior to sampling in both directions (equations shown in Figure 1 for MSS) shows the data are not sufficiently band-limited prior to sampling. Thus, the rectangular sampling can lead to considerable aliasing (or frequency ambiguity in sampled signals resulting from a low sampling rate), especially in the vertical (across-scan) direction. This is apparent when observing high frequency features (such as roads) in MSS pictures. TM data will be more aliased than MSS data in the horizontal direction since the sample spacing equals the instantaneous field-of-view (IFOV)[6] while for MSS is it less (IFOV/1.4).

Since the data are aliased, the interpolation function for rectification of scanner imagery may not be exactly given by Equation 1. Although the exact form of the interpolation function is beyond the scope of the present paper, it is clear from 1, 2, and 3 above that the function must be *separable*. It is also clear, from the fact that the data after resampling will be represented as new digital samples, that the function must be a close approximation to Equation 1 since the ideal prefilter[13] prior to sampling data is given by Equation 1. This fact is further supported by experimental evidence with MSS data and by numerous studies.[20-23]

SIMPLIFICATION OF TWO-DIMENSIONAL RESAMPLING

The resampling operation consists of convolving the digital samples $f(p,q)$ (where f is the picture intensity at integral values of p,q) with a two-dimensional kernel $g(x_1, x_2)$ (where g is given by Equation 1 for the band limited case). The intensity value at any x_1, x_2 is given by

$$f(x_1, x_2) = \sum_{p,q} f(p,q)\, g(x_1 - p, x_2 - q). \qquad (2)$$

Since g is separable, Equation 2 can be written as

$$f(x_1, x_2) = \sum_{q} g_2 (x_2 - q) \left[\sum_{p} g_1 (x_1 - p) f(p, q) \right].$$

Thus, the two-dimensional convolution is broken into a one-dimensional along-line convolution yielding the intermediate *function*

$$F(x_1, q) = \sum_{p} f(p, q)\, g_1(x_1 - p)$$

and another one-dimensional across-line convolution yielding the final *intensity*

$$f(x_1, x_2) = \sum_{q} F(x_1 - q)\, g_2(x_2 - q).$$

The process is illustrated pictorially for a four-pixel-wide kernel in Figure 2. The intermediate

points are obtained after the first interpolation (along x_1) and the final points after the second interpolation (along x_2) on the intermediate points. It is seen in this example that each output point requires four intermediate points (or in general N, where N is the kernel extent). The exception occurs when the output points have the same x_1 coordinate (i.e., they align vertically). Then the intermediate points can be shared by many output points, requiring only one intermediate point for each output point irrespective of N. When this is the case, one is performing two-dimensional resampling by two independent one-dimensional operations.

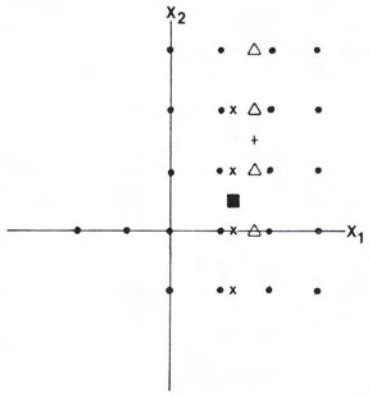

FIG. 2. Two-dimensional resampling in the separable kernel case. The first pass is performed in the x_1 direction to obtain the intermediate samples. The second pass is along the intermediate samples in the x_2 direction.

PRECISION RECTIFICATION

The mapping of pixel coordinates in precision rectification can be approximated by bilinear equations[2] whose coefficients are different in different blocks of the image. Denoting x_1 and x_2 as the input coordinates and y_1 and y_2 as the output coordinates, we have

$$x_1 = a_0 + a_1 y_1 + a_2 y_2 + a_3 y_1 y_2$$
$$x_2 = b_0 + b_1 y_1 + b_2 y_2 + b_3 y_1 y_2$$

Thus, the output image which consists of intensities at integer values y_1, y_2 is obtained by computing x_1 and x_2 with the above equation and then resampling at x_1, x_2 as explained previously. The transformation can be written in matrix form as (where the entry denoted by the dashed line is of no interest)

$$\begin{bmatrix} 1 \\ x_1 \\ x_2 \\ \text{---} \end{bmatrix} = \begin{bmatrix} 1 & 0 & 0 & 0 \\ a_0 & a_1 & a_2 & a_3 \\ b_0 & b_1 & b_2 & b_3 \\ 0 & 0 & 0 & 1 \end{bmatrix} \begin{bmatrix} 1 \\ y_1 \\ y_2 \\ y_1 y_2 \end{bmatrix}$$

It is possible to split the transformation* matrix into two matrices of the form

$$\mathbf{BA} = \begin{bmatrix} 1 & 0 & 0 & 0 \\ 0 & 1 & 0 & 0 \\ d_0 & d_1 & d_2 & d_3 \\ 0 & 0 & 0 & 1 \end{bmatrix} \begin{bmatrix} 1 & 0 & 0 & 0 \\ c_0 & c_1 & c_2 & c_3 \\ 0 & 0 & 1 & 0 \\ 0 & 0 & 0 & 1 \end{bmatrix}$$

where the c's and d's are easily evaluated from the a's and b's. Each of the transformation matrices acts only on rows or columns of data (i.e., are one-dimensional).

Thus, the geometric transformation can be split into two one-dimensional transformations. Whether the whole resampling process can be split into two one-dimensional operations depends on how well aligned vertically the pixels are after the first transformation.

Scanner data suffer from a variety of along-line errors due to the fact that data are collected line-by-line. In fact, the data samples cannot be considered samples of a two-dimensional signal (i.e., the above arguments do not apply) until distortions such as sensor offset and line length variation are removed[1]. These errors must be removed prior to two-dimensional processing. However, when one-dimensional processing applies, they can be incorporated into the first pass of the processing. Other systematic errors, such as Earth curvature, panoramic distortion, and scan nonlinearity are the same for all lines and thus cause no vertical misalignment after the first pass. Attitude errors are small and very slow changing[17,14,7] (10^{-2} deg/sec for Landsat C and much smaller for D and SPOT). They do not cause misalignments over the extent of typical resampling kernels (1 to 16 pixels). This slow change is also true of map projection distortions, such as UTM (most widely used). The only considerable vertical misalignment of pixels after the first resampling operation is due to Earth rotation correction. Earth rotation correction causes a uniform skew of the picture of less than 4°. In the image rotation section it is shown that this skew causes a small amount of aliasing in the across-scan direction. The fact that the original data are aliased in this direction justifies neglecting this small error during precision rectification.

IMAGE ROTATION

Before extending one-dimensional precision rectification to include large angle rotations (>10°) which are required for heading correction, it is essential to consider some sampling requirements for representing rotated images.

* The analysis can be extended to higher order equations and also to afine transformations.

The two-dimensional Fourier transform of an image ($f(\bar{x})$) and the image are related by

$$f(\bar{x}) = \frac{1}{(2\pi)^2} \int F(\bar{w}) \exp(+i\,\bar{w} \cdot \bar{x})\, d\bar{w} \qquad (3)$$

and

$$F(\bar{w}) = \int f(\bar{x}) \exp(-i\,\bar{w} \cdot \bar{x})\, d\bar{x} \qquad (4)$$

where $\bar{w} = (w_1, w_2)$ is the spatial frequency and $\bar{x} = (x_1, x_2)$ is the spatial coordinate. When the image is sampled at points

$$\bar{x} = l_1\,\bar{v}_1 + l_2\,\bar{v}_2$$

where l_1 and l_2 are integers and $\bar{v}_1$, $\bar{v}_2$ are sampling vectors (see Figure 3) the spectrum is duplicated at points

$$\bar{w} = m_1\,\bar{u}_1 + m_2\,\bar{u}_2$$

where m_1 and m_2 are integers and $\bar{u}_1$, $\bar{u}_2$ are vectors related to $\bar{v}_1$, $\bar{v}_2$

$$\begin{aligned} \bar{v}_i \cdot \bar{u}_j &= 2\pi \text{ for } i = j\ (i, j = 1, 2) \\ \bar{v}_i \cdot \bar{u}_j &= 0 \text{ for } i \neq j\ (i, j = 1, 2) \end{aligned} \qquad (5)$$

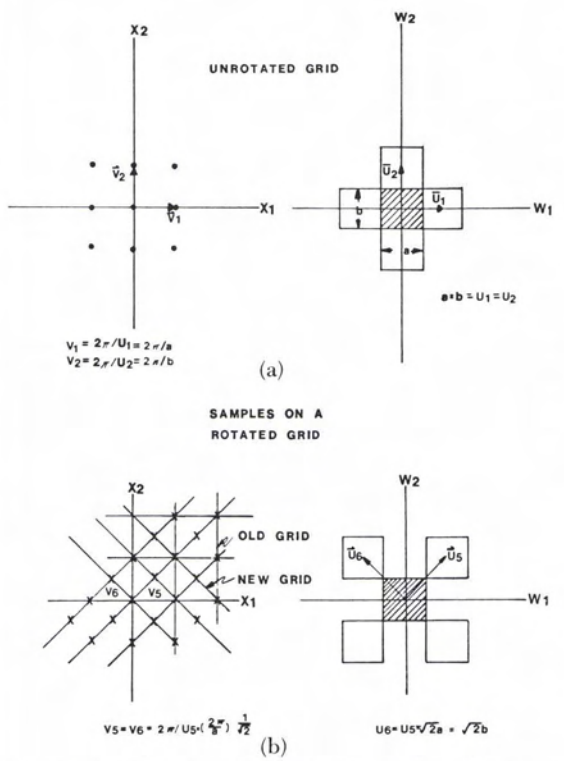

FIG. 3. Sampling two-dimensional signals with spectra contained within a square. (a) Rectangular sampling (optinal) along the spectra coordinates. (b) Rectangular sampling at 45° to the spectra coordinates. Twice as many samples are required in this case.

This is illustrated in Figure 3a for the case of rectangular sampling at the Nyquist rate. Now consider the case in which the sampling is to be along a rotated grid (45° will be used as an example for clarity) with respect to the original axis. This would produce samples along "scan lines" which are set 45° to the previous "scan lines". Since the samples are stored in matrix form, the image will be effectively rotated. The case is illustrated in Figure 3b. The sampling lattice is defined by points at the tips of vectors

$$\bar{v} = l_1\,\bar{v}_5 + l_2\bar{v}_6$$

which by relation (Equation 5) yield spectra repeated at positions

$$\bar{w} = m_1\,\bar{u}_5 + m_2\,\bar{u}_6$$

where $\bar{u}_5$ and $\bar{u}_6$ are as shown in Figure 3b. Clearly to avoid aliasing or spectra overlap (for square spectra example) we must have

$$|\bar{u}_5| = |\bar{u}_6| = \sqrt{2}\,a = \sqrt{2}\,b$$

where $a = b$ are the sides of the spectrum. This requires $\bar{v}_5$

$$|\bar{v}_5| = |\bar{v}_6| = 2\pi/|\bar{u}_5| = \frac{2\pi}{a}\frac{1}{\sqrt{2}}$$

to be $\sqrt{2}$ times smaller than $|\bar{v}_1| = |\bar{v}_2|$, the pixel separations of the unrotated images.

To adequately sample images with rectangular spectrum on a rotated grid, more samples are required than when sampling the image on a nonrotated grid. For a square spectrum the number of samples required doubles at 45°.

The above arguments affect the final pixel size (after precision rectification with heading correction) of corrected Earth resource data. Whatever the satellite heading, the rotation can always be reduced to one less than 45° by line inversion (180° rotation) or row/column transposition (90° rotation). Furthermore, the rotation required is seldom greater than 30° except at very high latitudes. With this in mind, Table 1 shows the envisioned pixel sizes (in metres) for future geocoded images from Landsat and SPOT.

EXTENSION OF ONE-DIMENSIONAL PROCESSING TO HANDLE LARGE ANGLE ROTATION

The procedure that one would like to follow to obtain pixels on a rotated grid by one-dimensional resampling is identical to the procedure used in precision rectification. It is illustrated in Figure 4. A one-dimensional resampling operation is performed along the scan line to obtain pixels on a line making an angle Θ (where Θ is the rotation angle) with the vertical. The second resampling operation now proceeds along this new line to obtain the output point on the rotated grid.

From previous arguments it is clear that the wrong intensity value is obtained since the inter-

TABLE 1. ENVISIONED PIXEL SIZES IN METRES FOR LANDSAT AND SPOT. THE SIZES ARE CHOSEN TO BE COMPATIBLE WITH IMAGE ROTATION REQUIREMENTS, WITH PRESENT MSS PRECISION PRODUCTS (50 m), AND WITH REQUIREMENTS FOR MERGING FUTURE DATA.

Sensor	Rotated Image
LANDSAT-D—MSS	50 × 50
—TM	25 × 25
SPOT—MLA	12.5 × 12.5
—panchromatic LA	6.25 × 6.25

mediate pixels do not align vertically after the first pass. Intuitively something is wrong because different rotation angles will yield different intensities at the same final output position.

The operation performed in this case differs from the correct one in that the filtering is not separable along the two orthogonal directions in which the data were sampled, but along two directions at an angle of 90 + Θ (for clockwise rotation).

It is useful to see what kind of a filter is being applied so as to gain an insight into how the error might be avoided. Examining the space frequency relations (Equation 5) one is lead to the conclusion that, to obtain a filter separable in the $\bar{v}_1$, $\bar{v}_2$ directions of Figure 4, one must choose a frequency domain filter separable along $\bar{u}_1$, $\bar{u}_2$ where $\bar{v}_1$, $\bar{v}_2$, $\bar{u}_1$, $\bar{u}_2$ obey relation (Equation 5). Consider the filter in Figure 5. This filter is of parallelogram

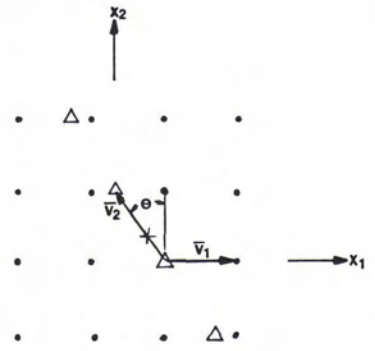

FIG. 4. Efficient (but improper) one-dimensional resampling to obtain pixels on a rotated grid. The first pass is in the $\bar{v}_1$ direction to obtain the intermediate samples. The second pass is along the intermediate samples in the $\bar{v}_2$ direction.

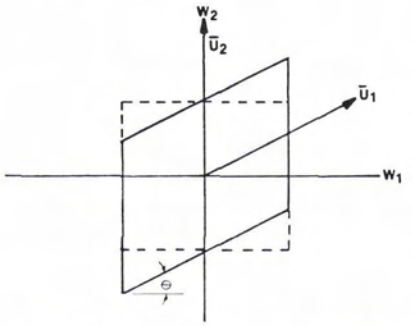

FIG. 5. Filter (solid line) applied in the case of resampling as in Figure 4. Dashed line shows extent of signal spectrum and the desired filter.

shape with sides parallel to the vectors $\bar{u}_1$ and $\bar{u}_2$. Consider also for simplicity that the filter is an ideal low-pass filter of this shape; that is,

$$G(\bar{w}) = G(\lambda_1 \bar{u}_1 + \lambda_2 \bar{u}_2) = \begin{cases} C & -\tfrac{1}{2} \leqq \lambda_1 \leqq \tfrac{1}{2} \\ & -\tfrac{1}{2} \leqq \lambda_2 \leqq \tfrac{1}{2} \\ 0 & \text{otherwise} \end{cases}$$

where λ_1 and λ_2 are running variables and C is a constant. The spatial domain form of this filter is given by the inverse transform of $G(\bar{w})$

$$g(\bar{x}) = \frac{1}{(2\pi)_2} \int G(\lambda_1 \bar{u}_1 + \lambda_2 \bar{u}_2)\, e^{i\,(\lambda_1 \bar{u}_1 + \lambda_2 \bar{u}_2)\cdot \bar{x}} d\bar{w}$$

since G is separable in $\bar{u}_1$ and $\bar{u}_2$ we have for the appropriate C[13]

$$g(\bar{x}) = \int_{-1/2}^{1/2} e^{i\,\lambda_1 \bar{u}_1 \cdot \bar{x}}\, d\,\lambda_1 \cdot \int_{-1/2}^{1/2} e^{i\,\lambda_2 \bar{u}_2 \cdot \bar{x}}\, d\,\lambda_2$$

$$= \frac{\sin \tfrac{1}{2}\, \bar{u}_1 \cdot \bar{x}}{\tfrac{1}{2}\, \bar{u}_1 \cdot \bar{x}} \cdot \frac{\sin \tfrac{1}{2}\, \bar{u}_2 \cdot \bar{x}}{\tfrac{1}{2}\, \bar{u}_2 \cdot \bar{x}}$$

In general, if the filter is not ideal, one still obtains the product of two functions of $(\bar{u}_1 \cdot \bar{x})$ and $(\bar{u}_2 \cdot \bar{x})$.

When performing the convolution (Figure 4) $\bar{x}$ is of the form

$$\bar{x} = \alpha \bar{v}_1 + \beta \bar{v}_2$$

where α and β are real variables, then

$$g\,(\bar{x}) = g(\alpha) \cdot g(\beta) = \frac{\sin \pi\, \alpha}{\pi \alpha} \cdot \frac{\sin \pi\, \beta}{\pi \beta}$$

Thus, the filter applied in a separable convolution along $\bar{v}_1$ and $\bar{v}_2$ is a parallelogram filter along $\bar{u}_1$ and $\bar{u}_2$ where $\bar{u}_1$ is orthogonal to $\bar{v}_2$ and $\bar{u}_2$ to $\bar{v}_1$. This filter is compared to the desired filter (dashed rectangular filter) in Figure 5. Clearly, use of the filter will lead to substantial loss of spatial frequencies from the original spectrum (within the dashed box) and substantial recovery and subsequent aliasing from neighbouring spectra. However, it is also clear how the error can be avoided.

If the data had been initially oversampled so as to separate the spectra in the frequency domain vertically, then the parallelogram filter would recover the correct spectrum. Thus, a third vertical pass to oversample the data prior to the two passes in Figure 4 is needed. In practice, one wants to make the first pass horizontally rather than vertically to remove things such as sensor offset, etc.

Figure 6 illustrates how precision rectification incorporating rotation is accomplished. First, a horizontal resampling operation is performed to oversample the data. Then, a vertical pass produces pixels at an angle Θ with the horizontal. Finally, another pass acts along these new "scan lines" to yield the final pixels.

The oversampling requirements are easily deduced from the geometry. For a square spectrum the pixel spacing during the first pass must be reduced by

$$\frac{1}{1 + \tan \Theta}$$

That is, for 45° the number of samples after the first pass doubles.

The first two resampling passes along the data are used to perform all the corrections previously discussed. These two passes are orthogonal and, except for the oversampling during the first pass and skewing during the second (which are easily accommodated in the bilinear equations), they are identical to the usual precision rectification passes. In particular, whatever resampling kernel is used in precision rectification can be used in these two passes. The final pass (which skews and scales the data) completes the rotation process to yield a geocoded image.

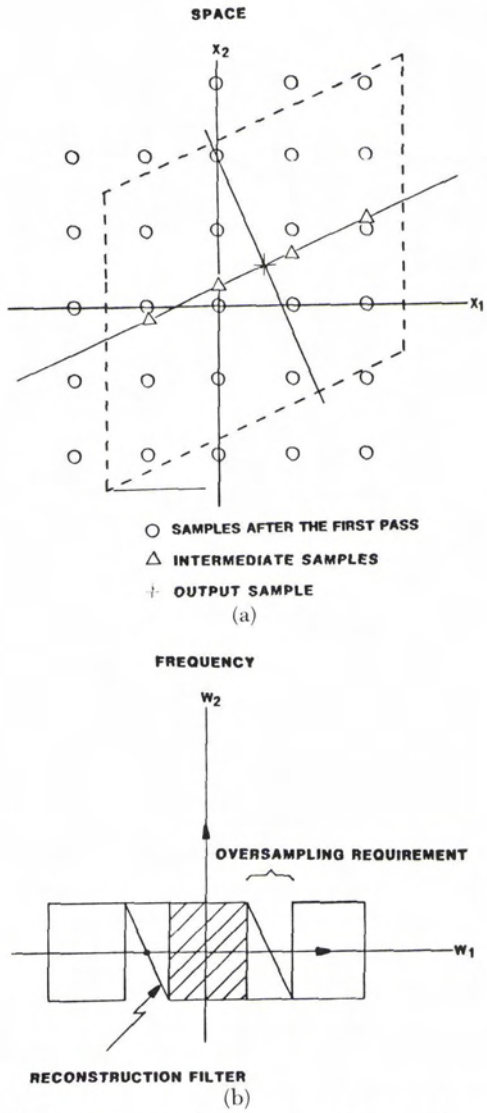

FIG. 6. Image rotation by three one-dimensional passes (first pass not shown). First pass has oversampled the data horizontally. Second pass, yielding intermediate points on the slanted line, is in the vertical direction. Final pass along the slanted line (new "scan line") yield samples on the rotated grid. (a) Operation in the spatial domain. (b) Operation in the frequency domain.

SIMULATION OF THE ROTATION ALGORITHM

The rotation algorithm was implemented in our Image Analysis System. The test data consisted of sine waves and Landsat MSS pictures. The sine waves demonstrated that accuracies of 1-bit RMS (in 256 levels) can be obtained with the three pass rotation method and that the two pass rotation method yields errors unacceptable to further machine processing of the data. The rotation of Landsat data illustrates the previous discussion well.

A 512 by 512 portion of band 6 of the Ottawa Scene (10747-15141), taken by Landsat, was rotated (40° using a 16-point kernel) with and without performing the initial oversampling. The fourier transform (FT) of the initial data and the rotated data are shown in Figure 7. Figure 7a shows the FT of the raw data. Figure 7b shows the FT of the data after rotation with three passes. The FT has the same shape but is rotated. The rotated FT is also smaller in order to fit within the same frequency cell as the FT of the original data (this is accomplished by enlarging the picture during the rotation process. See Figure 3). Figure 7c shows the FT of the data after rotation by the two pass method. It is clearly seen how this filter removes the corner of the original spectrum (i.e., the top and bottom of Figure 7b is not found in 7c). It is also seen how part of the next spectra is recovered (lower right and upper left Figure 7c). Finally, it can be seen where the next spectra repeated to the right and left aliases (i.e., upper right and lower left Figure 7c).

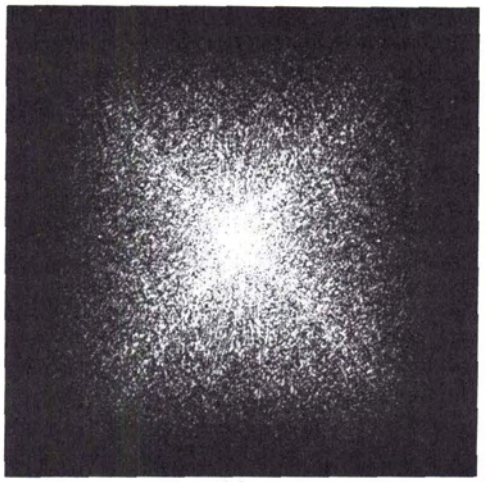

(a)

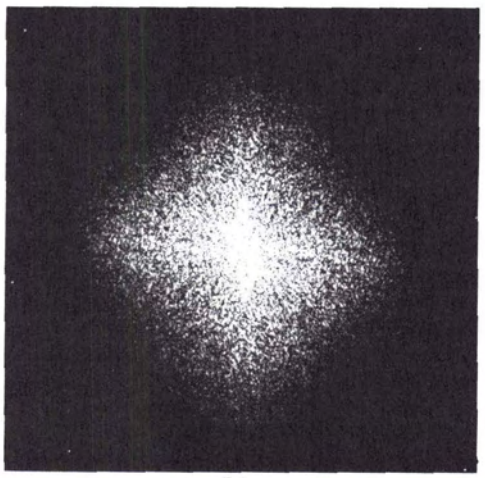

(b)

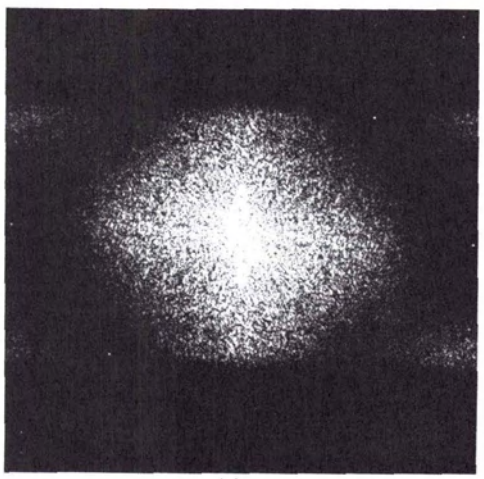

(c)

FIG. 7. Fourier transform (FT) of MSS data before and after rotation of 40°. (a) FT of the data prior to rotation. (b) FT of the rotated data with initial oversampling. (c) FT of the rotated data without the initial oversampling required.

CONCLUSIONS

One-dimensional processing of remote sensing data is desirable because

- Scanner data suffers from inherent one-dimensional distortions, some of which must be removed prior to two-dimensional processing;
- The processor is simpler and faster because the architecture is simple, the data access is easy, and the number of computations is less; and
- One-dimensional processing makes digital image rotation possible by eliminating the large memory requirements and slow data access which accompany two-dimensional digital image rotation.

In the future the last property (the possibility of performing image rotation fast) is perhaps the most important due to the increased number of sources of digital data.

It has been shown that Earth resource data from future sensors can be processed by a series of three one-dimensional operations to yield a geocoded (satellite independent) image.

ACKNOWLEDGMENT

The author wishes to thank Jerry Lim (MDA), M. Strome, E. Shaw, F. Guertin (CCRS), and R. Orth (MDA) for the many useful discussions during the course of this work. The author is especially indebted to Marshall Berger and Edd Lee for performing the software simulations. This work was supported in part by the Department of Industry Trade and Commerce Enterprise Development Program Project #534-3203.

REFERENCES

1. Van Wie, P., and M. Stein, A Landsat Digital Image Rectification System, *IEEE Transactions on Geoscience Electronics*, Vol. GE-15, No. 3, pp. 130-137, July 1976.
2. Rifman, S. S., Digital Rectification of ERTS Multispectral Imagery, *Third Earth Resources Technology Satellite-1 Symposium*, Vol. 1, NASA SP-351, pp. 1131-1142, 1974.
3. Bernstein, R., and H. Silverman, Digital Techniques for Earth Resource Image Data Processing, *Proceedings of the American Institute of Aeronautics and Astronautics, 8th Annual Meeting*, Vol. C21, AIAA Paper No. 71, October 1971.
4. Doyle, F. J., The Next Decade of Satellite Remote Sensing, *Photogrammetric Engineering and Remote Sensing*, Vol. 44, No. 2, pp. 155-163, February 1978.
5. Williams, O. W., Outlook on Future Mapping, Charting and Geodesy Systems, *Photogrammetric Engineering and Remote Sensing*, Vol. 46, No. 4, pp. 487-490, April 1980.
6. ———, *Proposal for Thematic Mapper (TM) Instrument System*, Executive Summary, Hughes Aircraft Co., prepared for NASA/GSFC, RFP No. 5-79160/229, August 1976.
7. ———, *Principal Characteristics of a National Satellite for Earth Observation, Project SPOT*, Centre National d'Etudes Spatiales (CNES), NTIS Order No. N78-24257, 55 pp., April 1978.

9. Colvocoresses, A. P., Multispectral Linear Arrays as an Alternative to Landsat D, *Photogrammetric Engineering and Remote Sensing*, Vol. 45, No. 1, pp. 67-69, January 1979.
9. Schnetzler, C. C., and L. L. Thompson, Multispectral Resource Sampler: An Experimental Satellite Sensor for the Mid-1980's, *Space Optics*, SPIE Vol. 183, pp. 255-262, 1979.
10. Colvocoresses, A. P., Proposal Parameters for Mapsat, *Photogrammetric Engineering and Remote Sensing*, Vol. 45, No. 4, pp. 501-505, April 1979.
11. Morganstern, J. P., R. F. Nalepka, and J. D. Erickson, Investigation of Thematic Mapper Spatial, Radiometric and Spectral Resolution, *Proceedings of the Eleventh International Symposium on Remote Sensing of Environment*, Vol. 1, pp. 693-701, April 1977.
12. Purll, D. J., *Consideration of Visible Photodetectors for LASS and COMSS Phase A Studies*, Final Report, Sira Institute Ltd., February 1979.
13. Petersen, D. P., and D. Middleton, Sampling and Reconstruction of Wave-Number Limited Functions in N-Dimensional Euclidean Spaces, *Information and Control*, Vol. 5, pp. 279-323, 1962.
14. ———, *Landsat D Position Determination and Correction Study*, Final Report, General Electric Co., NTIS Order No. N77-13496, 30 pp., November 1976.
15. Slater, P. N., A Re-Examination of the Landsat MSS, *Photogrammetric Engineering and Remote Sensing*, Vol. 45, No. 11, pp. 1479-1485, November 1979.
16. Lansing, J. C., and R. W. Cline, The Four and Five-Band Multispectral Scanners for Landsat, *Optical Engineering*, Vol. 14, No. 4, pp. 312-322, July/August 1975.
17. ———, *Landsat Data User's Handbook*, Revised Edition, U.S. Geological Survey, 1979.
18. Noorwood, V. T., Balance Between Resolution and Signal to Noise Ratio in Scanner Design of Earth Resource System, *Scanners and Imagery Systems for Earth Observation*, SPIE Vol. 51, 1974.
19. ———, *NASA, Advanced Scanners and Imaging Systems for Earth Observations*, NASA SP-335, 1973.
20. Simon, K. W., Digital Image Reconstruction and Resampling for Geometric Manipulation, *Proceedings of the Symposium on Machine Processing of Remotely Sensed Data*, West Lafayette, Indiana, pp. 3A-1-3A-11, June 1975.
21. Shlien, S., Geometric Correction, Registration, and Resampling of Landsat Imagery, *Canadian Journal of Remote Sensing*, Vol. 5, No. 1, pp. 74-89, May 1979.
22. Forman, M. L., *Interpolation Algorithms and Image Data Artifacts*, NTIS Order No. N78-10799, 20 pp., October 1977.
23. Ferneyhough, D. G., *Resampling Study*, NTIS Order No. E78-10014, 175 pp., March 1977.
24. ———, *Earth Resources Technology Satellite Spacecraft System Design Studies*, General Electric Co., NTIS Order No. N70-34454, April 1970.
25. ———, *Third Earth Resources Technology Satellite-1 Symposium*, Vol. 1, Sections A and B, NASA SP-351, 1974.
26. Landgrebe, D. A., L. L. Biehl, and W. R. Simmons, An Empirical Study of Scanner System Parameters, *IEEE Transactions on Geoscience Electronics*, Vol. GE-15, No. 3, pp. 120-129, July 1978.
27. ———, Line Scan Systems Frequency Space Analysis, *Earth Resources Technology Satellite Spacecraft System Design Studies*, General Electric Co., Book 3, Appendix 11.F, NTIS Order No. N70-34454, April 1970.
28. Biberman, L. M., Ed., *Perception of Displayed Information*, Plenum Press, New York, N.Y., 1973.
29. McGillem, C. D., T. E. Reimer, and G. Mobasseri, Resolution Enhancement of ERTS Imagery, *Proceedings of the Symposium on Machine Processing of Remotely Sensed Data*, West Lafayette, Indiana, pp. 3A-21-3A-29, June 1975.
30. McFadin, L. W., Application of Smart Sensor Techniques to a Solid State Array Multispectral Sensor, in *Remote Sensing of Earth from Space: Role of "Smart" Sensors*, (Ed.) R. A. Breckenridge, American Institute of Aeronautics and Astronautics, New York, N.Y., pp. 469-480, 1979.
31. Nowak, P., Application of Two-Dimensional Digital Filters to Multispectral Scanner Imagery, *5th Canadian Symposium on Remote Sensing*, Victoria, British Columbia, pp. 42-47, August 1978.
32. Rosenfeld, A., and A. C. Kak, *Digital Picture Processing*, Academic Press, New York, N.Y., 1976.
33. Stucki, P., Ed., *Advances in Digital Image Processing—Theory, Application, Implementation*, Plenum Press, New York, N.Y., 1979.

(Received 11 July 1980; accepted 18 February 1981; revised 6 April 1981)